Biochimica et Biophysica Acta 1837 (2014) 734–743

Contents lists available at ScienceDirect

Biochimica et Biophysica Acta

journal homepage: www.elsevier.com/locate/bbabio

Novel type of red-shifted chlorophyll *a* antenna complex from *Chromera velia*. I. Physiological relevance and functional connection to photosystems

Eva Kotabová [a,b,*,1], Jana Jarešová [a,b,1], Radek Kaňa [a,b], Roman Sobotka [a,b], David Bína [b,c], Ondřej Prášil [a,b]

[a] Institute of Microbiology ASCR, Centrum Algatech, Laboratory of Photosynthesis, Opatovický mlýn, 379 81 Třeboň, Czech Republic
[b] Faculty of Science, University of South Bohemia, Branišovská 31, 370 05 České Budějovice, Czech Republic
[c] Institute of Plant Molecular Biology, Biology Centre ASCR, Branišovská 31, 370 05 České Budějovice, Czech Republic

ARTICLE INFO

Article history:
Received 12 September 2013
Received in revised form 14 January 2014
Accepted 21 January 2014
Available online 28 January 2014

Keywords:
Chromera velia
Chromatic adaptation
Red-shifted chlorophyll
Light-harvesting complex
Photosystem II
Non-photochemical quenching

ABSTRACT

Chromera velia is an alveolate alga associated with scleractinian corals. Here we present detailed work on chromatic adaptation in *C. velia* cultured under either blue or red light. Growth of *C. velia* under red light induced the accumulation of a light harvesting antenna complex exhibiting unusual spectroscopic properties with red-shifted absorption and atypical 710 nm fluorescence emission at room temperature. Due to these characteristic features the complex was designated "Red-shifted *Chromera* light harvesting complex" (Red-CLH complex). Its detailed biochemical survey is described in the accompanying paper (Bina et al. 2013, this issue).
Here, we show that the accumulation of Red-CLH complex under red light represents a slow acclimation process (days) that is reversible with much faster kinetics (hours) under blue light. This chromatic adaptation allows *C. velia* to maintain all important parameters of photosynthesis constant under both light colors. We further demonstrated that the *C. velia* Red-CLH complex is assembled from a 17 kDa antenna protein and is functionally connected to photosystem II as it shows variability of chlorophyll fluorescence. Red-CLH also serves as an additional locus for non-photochemical quenching. Although overall rates of oxygen evolution and carbon fixation were similar for both blue and red light conditions, the presence of Red-CLH in *C. velia* cells increases the light harvesting potential of photosystem II, which manifested as a doubled oxygen evolution rate at illumination above 695 nm. This data demonstrates a remarkable long-term remodeling of *C. velia* light-harvesting system according to light quality and suggests physiological significance of 'red' antenna complexes.
© 2014 Elsevier B.V. All rights reserved.

1. Introduction

In an aquatic environment, photosynthetic organisms are distributed through the euphotic zone where the light conditions are variable and depend mainly on the absorption and scattering of water and various dissolved and particulate matter, including phytoplankton. In the oligotrophic areas, the light environment is driven by the optical properties of the water itself as the spectrum of light changes with depth. Red light and far-red light are strongly attenuated in the upper layer of the water column and blue light penetrates much deeper [1,2]. In optically more complex environments, such as shallow coastal waters, the spectrum of light is affected by the higher concentration of organic or inorganic particles and by the reflection from the sea floor [3,4]. Photosynthetic organisms that live in aquatic environments have developed strategies to sense and respond to variable ambient spectral conditions. In algae and protists, several sensory photoreceptors are used to detect the spectral quality of irradiance (for review, see [5]). The mechanisms responding to changes of the ambient spectral light quality were described as chromatic adaptation (CA) [6]. This phenomenon has been well documented for cyanobacteria (for recent review see [7]), but for eukaryotic organisms the current knowledge is rather inconsistent (see discussion in [8]). There are several studies describing CA in diatoms [8–13], dinoflagellates [14] and in colonies of coral reefs [1]. The CA in diatoms was identified as an inverse type [8], which is typically accompanied by compensatory changes within the photosystems at the thylakoid level. This is different in comparison to the complementary type of CA in cyanobacteria that involves preferential synthesis of major light-harvesting phycobilin pigments such as phycocyanin or phycoerythrin (reviewed in [7]).

Abbreviations: CA, chromatic adaptation; *C. velia-B*, *Chromera velia* grown on blue light; *C. velia-R*, *Chromera velia* grown on red light; Chl*a*, chlorophyll *a*; CLH(c), *Chromera* light harvesting (complex); ETR, electron transport rate; FCP, fucoxanthin chlorophyll *a*/*c* protein; LHC, light harvesting complex; $NPQ_{(\lambda)}$, non-photochemical fluorescence quenching (spectrally resolved); PAR, photosynthetically active radiation (400–700nm); PS I (II), photosystem I (II); Red-CLH(c), red-shifted *Chromera* light harvesting (complex); RT, room temperature; SRFI, Spectrally Resolved Fluorescence Induction

* Corresponding author at: Institute of Microbiology ASCR, Centrum Algatech, Laboratory of Photosynthesis, Opatovický mlýn, 379 81 Třeboň, Czech Republic. Tel.: +420 384 340 435; fax: +420 384 340 415.
E-mail addresses: kotabova@alga.cz (E. Kotabová), jaresova@alga.cz (J. Jarešová), kana@alga.cz (R. Kaňa), sobotka@alga.cz (R. Sobotka), bina@umbr.cas.cz (D. Bína), prasil@alga.cz (O. Prášil).
[1] E. Kotabová and J. Jarešová contributed equally to this study.

0005-2728/$ – see front matter © 2014 Elsevier B.V. All rights reserved.
http://dx.doi.org/10.1016/j.bbabio.2014.01.012

Diatoms possess several photoreceptors sensing both blue as well as red lights (see [2] and citations therein), however only the perception of blue light was found to be essential for acclimation to high light [13]. On the other hand, red light was reported to induce specific expression of Lhcf15, the fucoxanthin chlorophyll *a*/*c* protein, [13] and the appearance of the 710 nm PS II fluorescence emission at room temperature [9]. Although the mechanism(s) responsible for this red emission remain to be elucidated, available data suggests that photoprotection in diatoms is regulated not only by the light intensity but also by its quality and includes a large reorganization of antenna systems.

Focusing on the photosynthesis of coral reefs, the majority of photosynthetically active radiation (PAR) is absorbed by symbiotic algae of corals (zooxanthellae). The light environment inside the coral tissue and under the coral-reef invertebrates (e.g. ascidians) is strongly depleted in PAR, but enriched in far-red wavelengths [15–17]. Thus phototrophs associated with corals and didemnid ascidians had to extend their absorption capacity to the far-red region. This can offer a strategic advantage in niches where the PAR is limited [18]. For example, the ascidian associated cyanobacterium *Acaryochloris marina* uses chlorophyll *d* instead of chlorophyll *a* (Chl*a*) as a major pigment [19,20] that allows it to utilize available far-red light (700–750 nm). Recently, an even more far-red shifted chlorophyll *f* has been discovered in stromatolite samples [21]. The endolithic alga *Ostreobium* sp. is another oxygenic phototroph that can persist below a dense layer of other phototrophs due to extremely large number of red-shifted forms of Chl*a* [22–24]. The capacity to absorb light with wavelengths longer than 700 nm and the ability to utilize it for photosynthesis in *Acaryochloris* [25], *Acaryochloris*-like cyanobacteria [16] and in *Ostreobium* sp. [24] represents an important ecological advantage in coral-reef environment.

The role of red light absorbing pigments in the photochemistry of photosynthesis is still not clear. So far, the red forms of Chl*a*, discovered by Butler in the 1960s [26,27], were considered to be related mostly with the activity of photosystem I (PS I). Although relatively small in number (they form about 3–10% of the total chlorophylls), they have a pronounced effect on energy transfer and trapping in the PS I [28]. Nevertheless, they seem to be involved as well in PS II activity, as oxygen evolution induced by irradiance above 700 nm was also observed in Chl*a* containing phototrophs from regular habitats, such as green alga *Chlorella vulgaris* [29,30] and even for higher plants including sunflower, bean and spinach [31–33]. Despite clear evidence of far-red photochemistry [24,29–33], the role of red Chl*a* in PS II photochemistry is not generally accepted and there is only poor evidence for its presence in the PS II antennae. The only known exceptions are represented by the atypical association of PS I antenna Lhca1 with PS II in the endolithic alga *Ostreobium sp*. [23] and red-shifted antenna protein LHCb9 in the moss *Physcomitrella patens*, which possesses a typical motif for PS I antennae but associates with PS II [34,35]. However, the existence of such antennae in diatoms and brown algae was presumed for a long time [9,36–39].

In the present work, chromatic adaptation of *Chromera velia* and its physiological importance has been explored in detail. This recently discovered alga [40,41], together with *Vitrella brassicaformis* [42], represent a new phylum of algae called *Chromeridae* that are closely related to non-photosynthetic apicomplexan parasites [40,43–45]. *C. velia* is a coral associated alga [46,47] with highly efficient photosynthesis [48]. Its pigment composition is very simple, consisting of Chl*a*, isofucoxanthin-like carotenoid, violaxanthin and β,β-carotene [40]. Phylogenetically, the majority of light-harvesting complexes (LHCs) of *C. velia* form a separate cluster closest to dinoflagellate LHCs, and to the fucoxanthin chlorophyll *a*/*c* binding proteins (FCPs) of diatoms [49]. These complexes were designated recently as "*Chromera* light harvesting" (CLH) complexes because of their unique properties [50]. In addition, *C. velia* contains red alga-related PS I bound LHCs (PSI-LHCr) [49,50] and also LI818-like proteins [49] known to be induced during various stress conditions.

Here, we show that the prolonged growth of *C. velia* under monochromatic red light leads to the reversible appearance of an additional "Red *Chromera* light-harvesting" complex (Red-CLHc). This complex is assembled from a 17 kDa antenna protein and exhibits a remarkable red-shift in Chl*a* absorbance and fluorescence emission at room temperature. The far-red absorption/fluorescence nature of Red-CLHc is caused by a 17 kDa protein aggregation as shown in the accompanying paper [51]. This novel antenna complex is functionally connected to PS II and contributes to the effective light harvesting of far-red wavelengths.

2. Materials and methods

2.1. Culture conditions

C. velia (strain RM 12) was grown at 28 °C in artificial seawater medium with f/2 nutrient addition. Cells were kept in aerated glass tubes in semi-continuous batch growth with 24 h continuous irradiation. Panels made from LED strips were used for illumination with monochromatic red ($\lambda = 635$ nm) and blue ($\lambda = 460$ nm) lights of incident intensity of 20 μmol photons m^{-2} s^{-1}. All physiological measurements were performed with culture densities of 1.8–2.6 × 10^6 cells ml^{-1}. For biochemical analysis cells were harvested in late exponential phase.

2.2. Fluorescence and absorbance spectroscopy

Absorption spectra were measured in a glass cuvette using a Unicam UV 550 spectrophotometer (Thermospectronic, UK) equipped with an integration sphere. Absorbance was recorded with a scan rate of 30 nm/min with a 4 nm detection bandwidth.

Room temperature fluorescence emission spectra were measured in a cuvette with a SM-9000 spectrophotometer (Photon Systems Instruments, Czech Republic) for blue light excitation ($\lambda = 464$ nm) with a dark acclimated sample in the F_M (maximum fluorescence) state induced by a saturating pulse according to Kaňa et al. [52,53]. For the proper F710/F685 ratio calculation, the experimental data was deconvoluted using Origin Pro 8.0 "Peak Analyzer" (OriginLab, USA), using Gaussian curves. During the fitting procedure, only positions of peak maxima were restricted to a 4 nm range around the predicted maxima; all other parameters were set to be free for the minimization of procedure, driven by Chi-square (with 10^{-6} precision). The whole-cell emission spectra at varying excitation wavelengths (Fig. 9) were measured with a Spex Fluorolog-2 spectrofluorometer (Jobin Yvon, Edison, NJ, USA) using a slit width of 1.6 nm. The sample OD was <0.1 in the Chl*a* Q_y band. In the case of the far-red excitation (720 nm) the emission spectrum was composed of separate measurements of the uphill (<720 nm) and downhill (>720 nm) parts to avoid damage of the instrument by excitation radiation passing directly into the detector when excitation and emission monochromators were set to the same wavelengths.

77 K fluorescence emission spectra were measured using an Aminco–Bowman Series 2 spectrofluorometer (Thermo Fisher Scientific, USA) using standard instrument geometry. Diluted cell suspensions (in order to avoid fluorescence reabsorption) were placed in a sample holder and immersed in an optical Dewar flask filled with liquid nitrogen. The excitation was at 435 nm with a 4 nm slit width. The emission spectra were scanned with a 4 nm slit width. The instrument function was corrected by dividing the raw emission spectra by the simultaneously recorded signal from the reference diode.

2.3. Preparations of cell membranes

C. velia cells (200 mL, optical density at 750 nm ~ 0.5) were washed and resuspended in buffer containing 1 mL of 25 mM MES/NaOH, pH 6.5, 5 mM $CaCl_2$, 10 mM $MgCl_2$, and 25% glycerol. The concentrated cell suspension was mixed with 0.5 mL of glass beads (0.1 mm diameter) in a 2 mL Eppendorf tube and broken in a Mini-BeadBeater (BioSpec,

USA). The breaking cycle that includes 10 s bead-beating followed by 2-min cooling on ice was repeated 10-times. Membranes were separated from the cell extract by centrifugation (40,000 ×*g*, 20 min). The isolated membranes were resuspended in the working buffer and solubilized by gentle shaking with 1% dodecyl-β-maltoside at 10 °C for 1 h. Insoluble parts were removed by centrifugation (65,000 ×*g*, 20 min).

2.4. Denaturating and two dimensional electrophoresis

Membrane proteins prepared as described above were incubated with 2% SDS and 1% dithiothreitol for 1 h at room temperature and then separated on SDS-electrophoresis in a 12–20% linear gradient polyacrylamide gel containing 7 M urea [54]. Analysis of membrane complexes under native conditions was performed by a Clear-Native electrophoresis as described in Wittig and Schägger [55]. To record fluorescence emission spectra of antenna complexes, pigmented bands were cut from the native gel, placed on a laboratory-made holder and the chlorophyll fluorescence in the gel was measured by the spectrofluorometer (Aminco-Bowman Series 2, Thermo Fisher Scientific, USA) after excitation at 435 nm. To separate protein complexes in the second dimension, a gel strip from the Clear-native electrophoresis was incubated for 30 min in 25 mM Tris/HCl, pH 7.5 containing 2% SDS (w/v) and placed on top of the same denaturing gel system described earlier. Protein spots were stained with Coomassie Blue.

2.5. Cell composition

Cell numbers and size were determined with a calibrated Coulter Counter (Beckman Multisizer III) equipped with a 70 μm aperture. Specific growth rates (μ; d^{-1}) were calculated from $\mu = (\ln c - \ln c_0)/(t - t_0)$, where c is the cell concentration and t is time measured in days.

For cellular carbon and nitrogen determination, cultures were harvested onto precombusted (400 °C, 4 h) GF/F filters (Whatman, England) and frozen until analysis on a Micro-cube elemental analyzer (Elementar, Germany).

For pigment analysis, the aliquots of algal suspension were collected on GF/F filters (Whatman, England), soaked overnight at −20 °C in 100% methanol and subsequently disrupted using mechanical tissue grinder. Samples were kept on ice and in darkness to minimize pigment degradation. Filter and cell debris were removed by centrifugation (12,000 ×*g*, 15 min) and the extract was injected into an Agilent 1200 HPLC system equipped with a DAD detector. Pigments were separated using a Luna 3μ C8 column (100 × 4.60 mm; Phenomenex) at 35 °C with a linear gradient from 0.028 M ammonium acetate/methanol (20/80) to 100% methanol and with a flow rate set to 0.8 mL/min. Eluted pigments were identified according to absorbance spectra and the respective retention times and quantified at 440 nm with consideration of their different absorption at specific wavelengths. The molar extinction coefficients were used as follows (in L mol^{-1} cm^{-1}): 153×10^3 for violaxanthin (at 443 nm; solvent ethanol), 145×10^3 for zeaxanthin (at 450 nm; solvent ethanol), 141×10^3 for β-carotene (at 453 nm; solvent ethanol) [56] and 71.43×10^3 for Chl*a* (at 665 nm; solvent methanol) [57]. As the extinction coefficient for the isofucoxanthin-like pigment hasn't been yet determined, we used the coefficient of fucoxanthin calculated from $E^{1\%}_{1\,cm}$ used in Wright & Jeffrey [58] 105×10^3 (at 452 nm; solvent ethanol).

For chlorophyll quantification, we used the same extract, but measured the sample on a UV/VIS spectrophotometer (Unicam UV 550, Thermo Spectronic, UK). Chl*a* concentration was calculated according to Porra et al. [57].

2.6. Variable fluorescence measurements

Photosynthetic efficiency of PS II was calculated from variable Chl*a* fluorescence measured with a FL-3000 fluorometer (Photon System Instrument, Czech Republic). Samples were dark adapted for 20 min before applying low intensity measuring light (λ = 455 nm) for the detection of intrinsic fluorescence of the dark adapted sample (F_0). Subsequently a multiple turnover saturating flash (200 ms) was applied to measure the maximum quantum yield of photochemistry ($F_V/F_M = (F_M - F_0)/F_M$). Cells were then illuminated with an orange actinic light (λ = 625 nm; 480 μmol photons m^{-2} s^{-1}). Finally, after 2 min, another saturating flash was applied and non-photochemical quenching calculated as $NPQ = (F_M - F_M')/F_M'$ (Stern–Volmer formalism) where F_M and F_M' are the maximum fluorescence measured in the dark and light respectively. The effective quantum yield of PS II photochemistry (Genty's parameter; $\varphi_{PS\ II}$) was calculated as $\varphi_{PSII} = (F_M' - F_t)/F_M'$ and photochemical quenching as $qP = (F_M' - F_t)/(F_M' - F_0')$. The F_t was the actual fluorescence at given time excited by actinic light and F_0' was the minimal fluorescence of light adapted sample.

2.7. Spectrally Resolved Fluorescence Induction and non-photochemical quenching

The time courses of fluorescence induction at 685 nm (F685) and 710 nm (F710) presented in Fig. 7A were collected by means of the Spectrally Resolved Fluorescence Induction (SRFI) method described in detail by Kaňa et al. [52,53] using a FL-100 fluorometer (Photon System Instrument, Czech Republic) synchronized with a SM-9000 spectrophotometer (Photon Systems Instruments, Czech Republic). Presented fluorescence induction curves F685 and F710 were corrected to the intensity of excitation light used. The spectral changes in the non-photochemical quenching (NPQ) parameter were measured according to Kaňa et al. [59] with these modifications: NPQ was induced by a 2.5-minute long irradiation by strong blue light (1200 μmol photons m^{-2} s^{-1}, λ = 464 nm, Δλ ~ 20 nm). NPQ was calculated according to Stern–Volmer formalism for every wavelength.

2.8. Measurement of photosynthetic rates

The electron transport rate (*ETR*) was determined by measurement of fast repetition rate fluorescence using a modified FM 3500 fluorometer (Photon Systems Instruments, Czech Republic). After a 20 min dark adaptation a series of 100 sub-saturating flashes (λ = 463 nm, 1.5 μs) inducing a single turnover flash for sequential PS II closure, was applied. This was done for the 11 levels of amber (λ = 590 nm) actinic light intensities (0–1340 μmol photons m^{-2} s^{-1}). The data was fitted and ETR calculated according to citations and equations described in Quigg et al. [48].

Oxygen evolution was measured using a Clark-type electrode (Theta 90, Czech Republic) in the presence of 1 mM sodium bicarbonate. The rate of gross oxygen evolution was calculated from the slope of net O_2 evolution measured at saturating irradiance plus the slope of respiratory O_2 utilization measured in the dark just after light exposure. For standard measurement, cells were irradiated with white actinic light (KL1500, SCHOTT, USA). To test if long wavelength quanta could support the oxygen evolution in *C. velia* we used a 695 nm longpass filter (FGL695, Thorlabs, USA); in this case the irradiance was not saturating. The oxygen evolution rate was normalized to the Chl*a* content.

Photosynthetic carbon fixation was assessed from incorporation of radioactive $H^{14}CO_3^-$ using the protocol described previously [48]. The samples were incubated with the ^{14}C isotope in the laboratory-built photosynthetron [60] for 40 min at 28 °C. Disintegrations per minute were counted on a calibrated Tri-Carb 2810 TR Liquid Scintillation Analyser (PerkinElmer, USA). The total dissolved CO_2 in the media was determined by alkalinity titrations. The carbon fixation rate was normalized to the Chl*a* content. All measurements of photosynthetic rates were performed at 28 °C.

3. Results

3.1. Spectroscopic analysis of C. velia cells during chromatic adaptation

The absorption spectra of whole cells reflected the typical pigment composition of *C. velia*, which contains Chl*a*, violaxanthin, β-carotene and an isofucoxanthin-like pigment [40]. Interestingly, the cell culture grown under red light (hereafter *C. velia-R*) showed a red-shifted absorbance with maximum around 705 nm (Fig. 1) that was completely missing in the culture grown at blue light (*C. velia-B*). The presence of the red-shifted pigments in *C. velia-R* was also readily detectable in fluorescence emission spectra recorded at room temperature (RT). As shown in Fig. 2A, *C. velia-R* exhibited two fluorescence emission bands at RT; the typical 688 nm emission of the PS II core was accompanied by an additional dominant emission band at 710 nm (Fig. 2A), reflecting emission from pigments absorbing above 700 nm. As expected, the emission of red-shifted chlorophylls was even more visible at low temperatures (Fig. 2B). *C. velia-B* had a maximum of the 77 K fluorescence at 690 nm, while *C. velia-R* at 717 nm. Although *C. velia* was already shown to rearrange its fluorescence emission as a response to light intensity [48], this data suggests that the light quality has a much greater effect.

To further explore the chromatic adaptation of *C. velia* to red light the RT F710 emission band was employed as a marker. Particularly, to monitor kinetics of chromatic adaptation to light quality we follow changes in the RT fluorescence ratio F710/F685 after shifting *C. velia-B* to the red light and vice versa. As shown in Fig. 3, upon the shift from red to blue light the fluorescence maximum at 710 nm completely disappears within several days. The relative F710 decline can already be observed after 18 h, during the following two days the F710/F686 ratio dropped to 50% and finally became negligible after about two weeks of keeping cells under blue light. The opposite process is significantly slower. Upon the shift of *C. velia-B* to red light we observed a 2 day long lag phase before the F710 emission emerged (Fig. 3). After this period, the F710 emission developed gradually and reached its maximum within 18 days. When the F710 first appeared in *C. velia-B* shifted to red light, the *C. velia-R* culture shifted to blue light already showed a 50% decline of F710. Our data clearly shows that the chromatic adaptation of *C. velia* to red light comprises a relatively slow accumulation of red-shifted pigments and this process is reversible on blue light with faster kinetics.

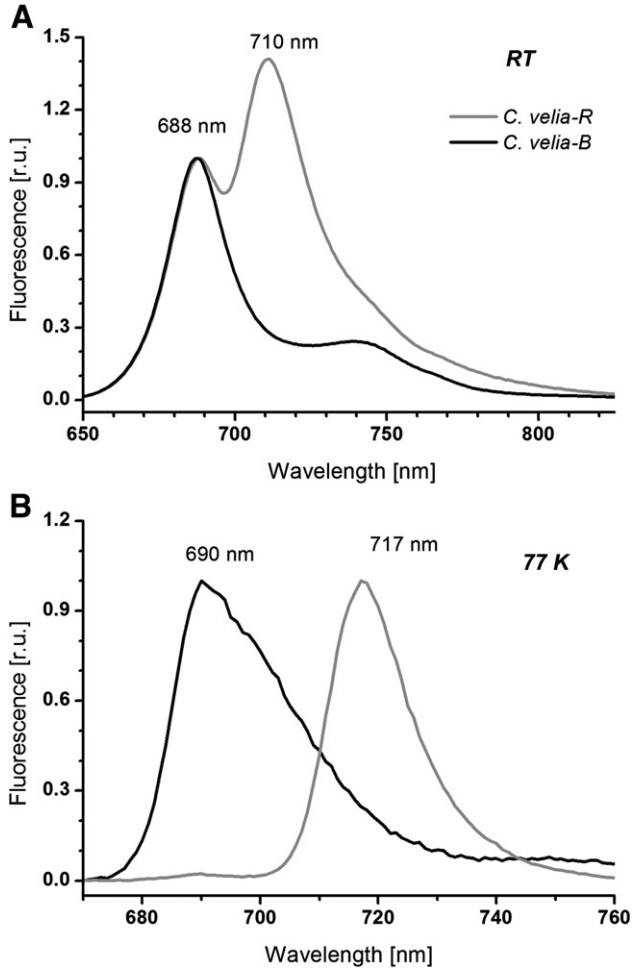

Fig. 2. Fluorescence emission spectra of *C. velia* grown under red (*C. velia-R*) and blue (*C. velia-B*) light. *Panel A* represents fluorescence emission spectra measured at room temperature (RT); *Panel B* shows fluorescence emission spectra measured at low temperature (at 77 K). Fluorescence was induced by excitation to Chl*a* at 464 nm (RT) and at 435 nm (77 K). The presented fluorescence emission spectra were normalized to the fluorescence maxima (at 688 nm for RT fluorescence and at appropriate maximum for 77 K fluorescence). Data represents typical curves.

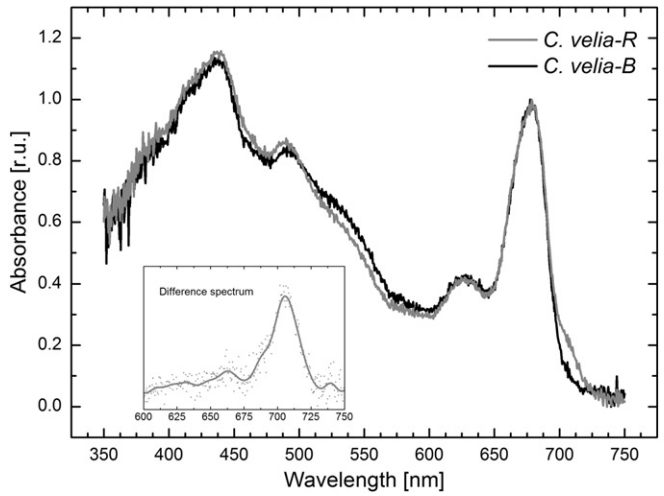

Fig. 1. Absorption spectra of whole cells of *C. velia* grown under red (*C. velia-R*) and blue (*C. velia-B*) light. The spectra were normalized to Chl*a* absorption maximum at 678 nm. *Inset*: the difference spectrum between red and blue light adapted culture.

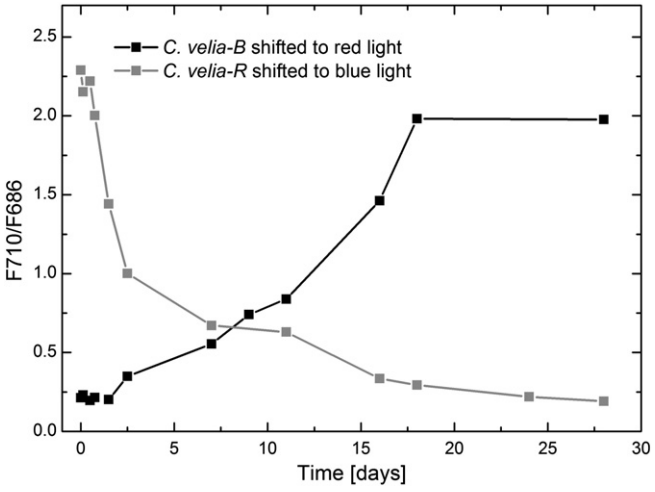

Fig. 3. Time course of *C. velia* chromatic adaptation upon shift from blue to red growth light and vice versa. The process is characterized based on RT fluorescence ratio F710/F686. The F710 fluorescence emission maximum reflects amount of red-shifted chlorophylls, the F686 fluorescence emission maximum reflects fluorescence of photosystem II. Ratios were calculated after spectra deconvolution.

3.2. Re-organization of pigment protein complexes

Observed appearance of red absorbing chlorophylls in *C. velia* acclimated to red light could arise from a rearrangement of existing pigment complexes or, alternatively, from the accumulation of new chlorophyll-binding complex(es). In order to distinguish between these possibilities we first analyzed the composition of membrane proteins by denaturating SDS electrophoresis (Fig. 4). Interestingly, cells acclimated to red or blue light had virtually the same pattern of membrane proteins except for the presence of a protein with a mass of approximately 17 kDa in the *C. velia-R* sample. To obtain more details about the 17 kDa protein, we analyzed membrane protein-complexes by two dimensional electrophoresis. Solubilized complexes were first separated by clear-native-electrophoresis (CN-PAGE in Fig. 5). In the case of both samples (*C. velia-R* and *C. velia-B*) pigmented high molecular mass complexes can be recognized on the top of the CN-PAGE. As reported recently, these bands on the top of the gel represent a stable, megadalton super-complex(es) of photosystems and antennae proteins (Fig. 5, [61]), which also explains why typical bands of PS I and PS II are not observed (Fig. 5). Further, in both samples, two broad antenna bands run on the bottom of the electrophoretic gel corresponding to the recently characterized CLH antenna [50]. We were able to distinguish two CLH antenna complexes different in molecular masses; the *Chromera* light harvesting complex I (CLHc I) and complex II (CLHc II) that represent smaller CLH trimers and larger CLH oligomers respectively, as described in Tichý el al. [50]. In *C. velia-R* variant, the CLHc II is clearly more yellowish and has a stronger intensity of Chl*a* fluorescence (Fig. 5), indicating some changes due to chromatic adaptation to red light. Importantly, the presence of a new antenna complex, migrating a bit faster on the CN-PAGE than the CLHc I, is apparent from the chlorophyll 'in gel' fluorescence (Fig. 5).

Individual subunits of observed pigmented complexes were further resolved in a second dimension by SDS electrophoresis (Fig. 5). Denaturing gel showed that both CLH complexes in *C. velia-B* cells are composed from at least two antenna proteins with similar molecular masses around 20 kDa and 22 kDa, and thus likely representing two oligomeric states of the same antenna complex. The 17 kDa protein, specific for *C. velia-R* sample, migrates between CLH complexes as an independent antenna protein and co-migrates with observed chlorophyll fluorescence and the yellowish band on CN-PAGE (Fig. 5). We have thus tentatively designed this antenna complex as a novel Red-CLH complex. Intriguingly, all individual antenna proteins including the 17 kDa protein seem to dissociate during electrophoresis from the large complex migrating close to the top of the gel. However, no chlorophyll fluorescence of this supercomplex was detected (Fig. 5), which implies a very efficient fluorescence quenching, most probably due to the presence of PS I [61].

A comparison of the room temperature fluorescence spectra of the CLH complexes clearly showed that only the Red-CLH complex exhibits the red-shifted emission band (710 nm; Fig. 6) typical for *C. velia-R* intact cells (see Fig. 2A). Moreover, the size of the Red-CLH on CN-PAGE, just above the CLHc I indicates that the 17 kDa protein forms an aggregate larger than trimers described in Tichý et al. [50], despite its lower molecular mass compared to the components of CLH. Further analysis of the purified Red-CLH complex describing its pigment composition, spectroscopic properties and phylogenetic origin is provided in the accompanying paper [51].

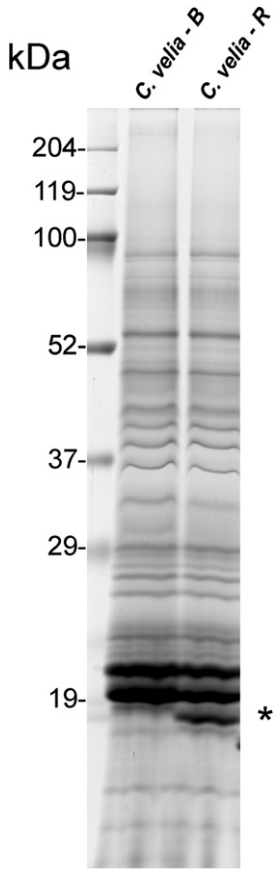

Fig. 4. SDS-electrophoresis of membrane proteins isolated from *C. velia* grown under monochromatic blue (*C. velia-B*) and red (*C. velia-R*) light. A 17 kDa antenna protein induced specifically by red light is marked by asterisk.

3.3. Physiological consequences of chromatic adaptation in C. velia

The effect of pigment-protein re-organization during chromatic adaptation on the physiology of photosynthesis was further explored in detail. The *C. velia-R* and *C. velia-B* had similar specific growth rates (μ); the μ of *C. velia-R* was only 7% lower compared to *C. velia-B* (Table 1). We have observed no changes in cell size or cellular carbon per nitrogen (C/N) ratio (Table 1). Growth under red light resulted in a higher concentration of photosynthetic pigments per cell; Chl*a* concentration increased by 11% (Table 1) and relative content of violaxanthin by 18% (both per total pigments as well as per Chl*a*; Table 2). Interestingly, an opposite effect (de-pigmentation) is caused by red light in diatom species, e.g. in *Phaeodactylum tricornutum* [13] and *Haslea ostrearia* [8]. We observed no variations in photosynthetic rates of *C. velia-R* and *C. velia-B* when calculated per Chl*a* as differences in oxygen evolution (representing light reactions) and carbon fixation (dark reactions) were insignificant (Fig. 8A, Table 3). The only significant difference we found was for the electron transport rate which was slower by 21% in *C. velia-R* (Table 3). This is in line with the data presented for diatoms *P. tricornutum* [13] and *H. ostrearia* [8]. Differences in the maximal efficiency of PS II photochemistry in the dark were minimal; F_V/F_M was 0.54 and 0.58 for *C. velia-R* and *C. velia-B* respectively (Table 4). The effective quantum yield of PS II on light, φ_{PSII} (Genty parameter), was very low for both variants (~0.06, Table 4). Such a low value of φ_{PSII} is typical for *C. velia* photosynthesis and does not signify low efficiency or impairment of PS II, but seems to be related to a shared antennae pool between PS I and PS II [48]. This is in agreement with large aggregates of photosystems and antenna proteins observed on CN-PAGE (Fig. 5, [61]) indicating a firm interconnection among components of photosynthetic apparatus. In contrast to diatoms [13], we did not observe a dramatic difference in NPQ between *C. velia* grown under red or blue light. The NPQ of *C. velia-R* was only by 13% lower compared to *C. velia-B* (Table 4). In summary, we did not observe a marked effect of chromatic adaptation of *C. velia* on physiology of photosynthesis. Red light grown cells grew a bit slower that could probably be related to the formation of

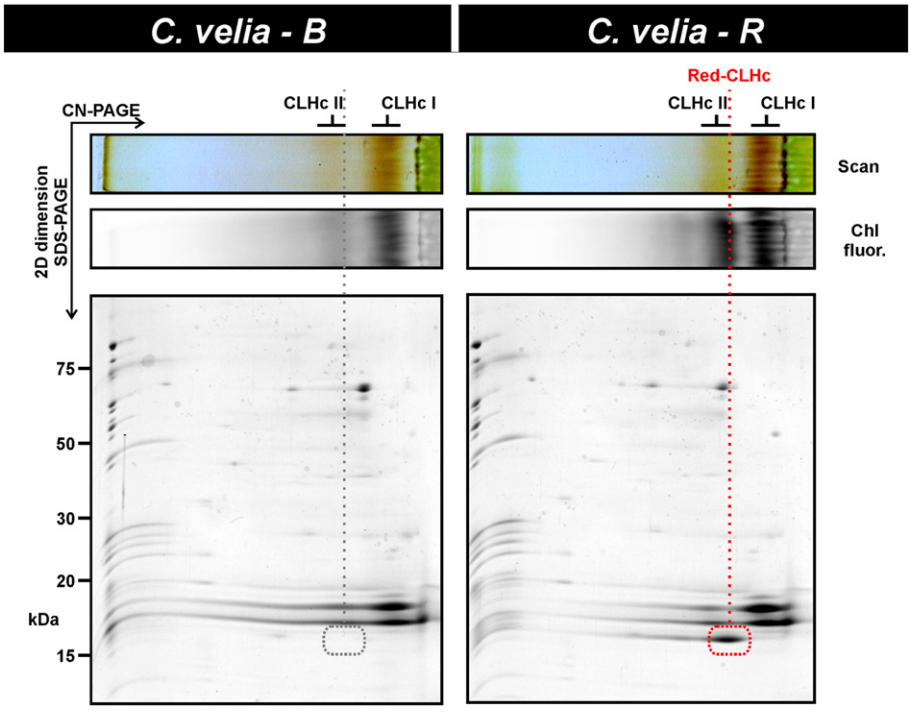

Fig. 5. 2D electrophoresis of membrane protein complexes isolated from *C. velia* grown under monochromatic blue (*C. velia-B*) and red (*C. velia-R*) lights. Membrane proteins were solubilized by dodecyl-β-maltoside and separated in a first dimension by clear-native electrophoresis (CN-PAGE). The native gels were scanned in true colors ("Scan"); Chl*a* fluorescence ("Chl fluor.") was detected using LAS 4000 (Fujifilm Life Science, USA) with 460 nm excitation wavelength and 670 nm long pass filter. The protein complexes resolved on the CN-PAGE were further separated in the second dimension by denaturing gel (SDS-PAGE) and stained by Coomassie Blue. The positions of typical light harvesting complexes CLHc I and CLHc II are marked by black lines above CN-PAGE. The red-shifted light harvesting antennae complex (Red-CLHc) specific for *C. velia-R* is marked by red line, the putative position of this complex in *C. velia-B* is highlighted by gray line. The 17 kDa antenna protein co-migrating with the Red-CLHc is red-circled.

the new 17 kDa protein (see Figs. 4 and 5). *C. velia-R* was also more pigmented, had less efficient PS II in dark (F_V/F_M) and substantially slower ETR. However, the integrated physiological parameters, like the rates of photosynthetic carbon fixation and oxygen evolution were similar for both variants. All these above mentioned adaptations, including synthesis of new 17 kDa protein, allow for successful chromatic adaptation of *C. velia* to red light.

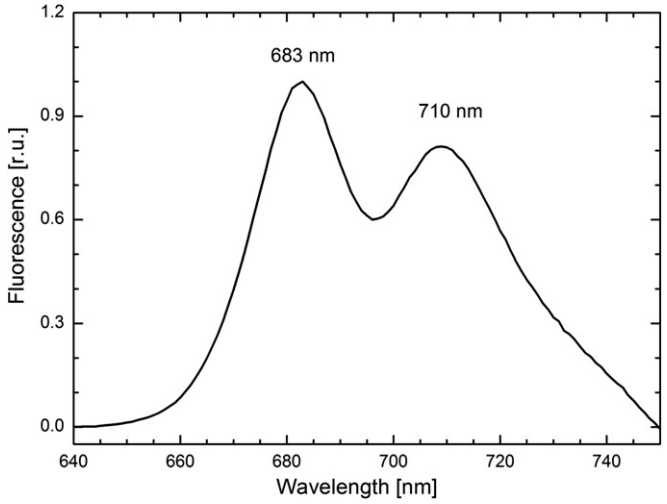

Fig. 6. Room temperature fluorescence emission spectra of the Red-CLH complex isolated from *C. velia-R* cells by CN-PAGE (see Fig. 5). This pigment–protein complex contains the 17 kDa protein as it is apparent from the 2D gel (see Fig. 5).

3.4. Organization of the thylakoid membrane. The red-shifted antenna delivers excitations to PS II

The excitation energy flow between the red antenna and photosystems was investigated by means of Spectrally Resolved Fluorescence Induction (SRFI) method, oxygen evolution measurement and steady state fluorescence spectroscopy. As can be seen in Fig. 7A, excitation into the Chl*a* at 464 nm produced very similar fluorescence induction curves for fluorescence signals at 685 nm (F685) reflecting typical PS II and at 710 nm (F710) reflecting far-red antenna. This observation clearly implies that the red-antenna complex (Red-CLHc in Fig. 5) is functionally connected with PS II. Calculating the spectrally resolved NPQ (NPQ_λ) according to Kaňa et al. [59] we have noticed a significant rise of NPQ_λ in the region of 700–750 nm with the maximum between 710 and 720 nm in the *C. velia-R* variant (Fig. 7B) implying that red antenna is somehow involved in excess energy dissipation via NPQ.

It was already mentioned that the oxygen evolution rates were comparable for both *C. velia-R* and *C. velia-B* cultures when measured with standard white actinic light (Fig. 8A, Table 3). To test the physiological relevance of energy transfer between the red antenna and PS II, we

Table 1
Cellular response of *C. velia* grown under red (*C. velia-R*) and blue (*C. velia-B*) continuous light.

	μ [d^{-1}]	Cell size [μm]	C/N [mol/mol]	Chlorophyll/cell [pg $cell^{-1}$]
C. velia-R	0.127 ± 0.002	7.1 ± 0.0	5.5 ± 0.1	0.82 ± 0.05
C. velia-B	0.137 ± 0.001	7.0 ± 0.1	5.5 ± 0.1	0.74 ± 0.04
p	$p < 0.05$ ($n = 2$)	n.s. ($n = 3$)	n.s. ($n = 3$)	

Table 2
Pigment composition of *C. velia* grown under red (*C. velia-R*) and blue (*C. velia-B*) continuous light.

	Chlorophyll/total pigments [mol/mol]	Violaxanthin/total pigments [mol/mol]	Isofucoxanthin/total pigments [mol/mol]	Violaxanthin/Chl*a* [mol/mol]	Isofucoxanthin/Chl*a* [mol/mol]
C. velia-R	0.38 ± 0.04	0.20 ± 0.01	0.40 ± 0.03	0.52 ± 0.05	1.06 ± 0.12
C. velia-B	0.39 ± 0.04	0.17 ± 0.01	0.42 ± 0.04	0.44 ± 0.05	1.07 ± 0.12
p	n.s. (n = 5)	p < 0.001 (n = 5)	p < 0.05 (n = 5)	p < 0.01 (n = 5)	n.s. (n = 5)

Table 3
Photosynthetic rates of light and dark reactions in *C. velia* grown under red (*C. velia-R*) and blue (*C. velia-B*) continuous light.

	Electron transport rate [μmol electrons mg chla^{-1} h^{-1}]	Oxygen evolution rate [μmol O_2 mg chla^{-1} h^{-1}]	Carbon fixation rate [mg C mg chla^{-1} h^{-1}]
C. velia-R	643 ± 39	206 ± 19	1.88 ± 0.08
C. velia-B	818 ± 79	214 ± 8	1.79 ± 0.04
p	p < 0.001 (n = 12)	n.s. (n = 3)	n.s. (n = 3)

have measured oxygen evolution under far red light (>695 nm). As seen in Fig. 8B, *C. velia-R* cells showed a marked increase in oxygen evolution rates compared to the *C. velia-B* culture, unambiguously demonstrating that the energy captured by the red-antenna complex is capable of driving the PS II photochemistry. This result is in agreement with earlier observations in the green alga *Ostreobium* sp. [24]. Also like in *Ostreobium* sp., the above described observation indicates that the PS II photochemistry relies on the (thermally activated) uphill energy transfer.

To further study the excitation energy partitioning in the red-light adapted *C. velia*, we employed steady state fluorescence spectroscopy at room temperature. Fig. 9 presents a comparison of steady state emission spectra of *C. velia-R* cells measured with excitation into the Chl*a* Soret band (435 nm), violaxanthin (490 nm), iso-fucoxanthin-like carotenoid (540 nm) and the far-red Chl*a* band (720 nm) as indicated in the figure inset. In the case of the far-red excitation, the emission detected in the range of 620–720 nm represents the anti-Stokes emission from thermally populated states; as expected, no such emission was observed in measurements done at cryogenic temperatures (data not shown). The almost perfect agreement between the spectra recorded in the Stokes (excitation energy above the fluorescence) and anti-Stokes modes suggests that the light-harvesting complexes in the membrane of *C. velia* cells act as a unified pool of pigments in which the excitation is distributed according to the thermal equilibrium. This implies no spatial hindrance to excitation migration and consequently no separation into structural domains. It thus follows that the energy captured by the red-antenna is distributed to both PS II and PS I which share a common antenna pool. This represents a limiting case of earlier observations in *C. velia* [48] that also indicated certain extent of antenna sharing between the photosystems.

4. Discussion

Chromerids, close relatives of apicomplexan parasites [40,43], are known to be associated with coral reef environments, predominantly off-shore tropical and warm subtropical waters [62]. *C. velia* is the first chromerid described [40,41] and is able to operate highly efficient and adaptive photosynthesis [48]. However, it has not been known how it can adapt to the specific spectral conditions of its environment.

Phototrophic organisms associated with coral reefs often exhibit a red shift of the absorption of their antenna complexes. This kind of adaptation has been shown to increase the light harvesting potential of PS II under conditions where the intensity of PAR around 680 nm is absorbed by the overlying layers of phototrophs [63]. Moreover, in aquatic environments, the problem of shading is exacerbated by the fact that water itself is a strong absorber in the region above 700 nm. Hence combination of filtering by the water column and Chl*a*-containing phototrophs leaves just a rather narrow window around 710 nm. Indeed, in this spectral region the most of red-shifted absorption bands are found. For instance, the cyanobacterium *A. marina*, achieves red-shifted absorption using an unique pigment, chlorophyll *d*, with absorption maximum in the 700–720 nm region [18]. The green alga *Ostreobium* sp. employs the red shifted Chl*a* localized in the Lhca complexes that are connected to PS II rather that PS I [22,23]. The same limitations in the availability of PAR hold also for benthic diatoms such as *Pheodactylum and Nitzschia* [64] that are also known to express red-shifted Chl*a*-containing antenna complexes. Identity of the diatom red-shifted complexes has not been elucidated although the available data indicate association with the Lhcf/FCP family [9,13]. In the present study and the accompanying paper [51] we demonstrate that *C. velia* utilizes a novel red-shifted antenna complex, Red-CLHc (Fig. 5) without close relation to both the Lhca proteins and the antenna complexes of diatoms [51].

Our biochemical analysis has shown that in *C. velia* the chromatic adaptation to red light is accompanied by the accumulation of a 17 kDa protein assembled into the Red-CLH complex. This antenna complex has unusual spectroscopic properties with atypical, red-shifted absorption at 705 nm (Fig. 6) and corresponding RT fluorescence emission at 710 nm (Figs. 2 and 6). The red-shifted absorption/fluorescence of Red-CLHc is not an internal property of the 17 kDa protein itself but is caused by 17 kDa protein aggregation into an oligomer (see the accompanying paper [51]). The similar spectroscopic behavior including stimulation of absorption above 700 nm and F710 fluorescence signal at RT has been documented for diatoms *P. tricornutum* and *Nitzschia closterium* grown on weak red light [9]. The F710-like emission was also reported in several strains of phaeophytes [39].

Red chlorophylls are generally considered to be associated with PS I in cyanobacteria or with PS I antennae of plants (see e.g. [28,65,66]). It is expected that these red-shifted chlorophylls represent chlorophyll

Table 4
Photosystem II photochemistry of *C. velia* grown under red (*C. velia-R*) and blue (*C. velia-B*) continuous light.

	F_V/F_M	φ PSII	1-qP	NPQ
C. velia-R	0.541 ± 0.002	0.061 ± 0.001	0.746 ± 0.006	1.07 ± 0.02
C. velia-B	0.576 ± 0.004	0.057 ± 0.006	0.772 ± 0.018	1.23 ± 0.01
p	p < 0.001 (n = 3)	n.s. (n = 3)	n.s. (n = 3)	p < 0.001 (n = 3)

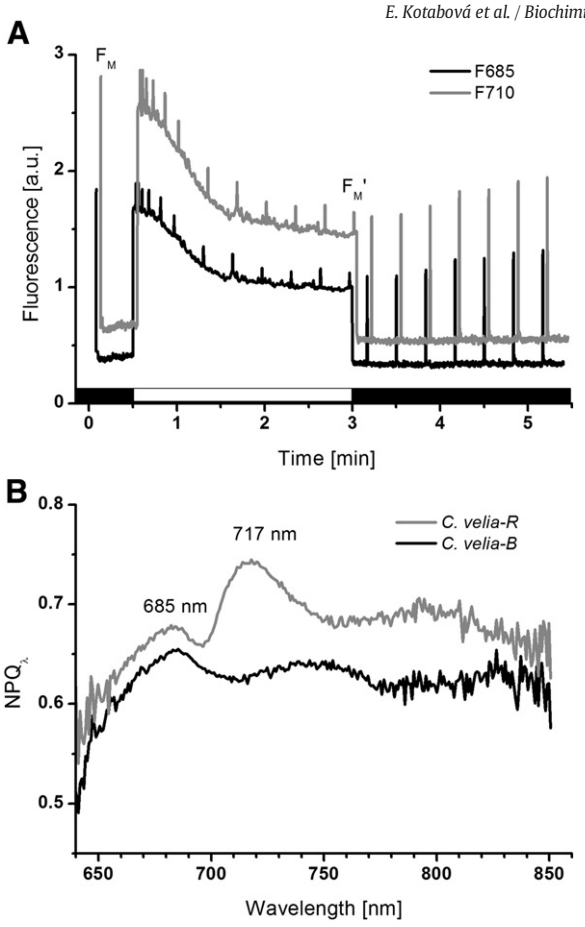

Fig. 7. Spectrally Resolved Fluorescence Induction (SRFI) measured with *C. velia* adapted to red (*C. velia-R*) or blue (*C. velia-B*) monochromatic growth irradiance. *Panel A*: Time course of Chl*a* fluorescence quenching analysis of *C. velia-R* that was detected simultaneously for all emission wavelengths under the excitation at 464 nm. The fluorescence signals at 685 nm (F685; reflecting typical PS II) and at 710 nm (F710; reflecting far-red antenna) are presented. Cells were dark adapted for 20 min before application of saturating pulse to measure the maximal fluorescence (F_M). Then actinic light was applied for 150 s (see white bar) and the maximal fluorescence on light was measured (F_M'). The recovery after light period was measured for following 150 s (see black bar). The signals of F685 and F710 were corrected for different intensities of excitation light used during protocol. *Panel B*: The data from SRFI were employed to calculate the spectrally resolved non-photochemical quenching ($NPQ_\lambda = (F_{M\lambda} - F_M'_\lambda)/F_M'_\lambda$) for both *C. velia-R* and *C. velia-B*. Data represent typical curves.

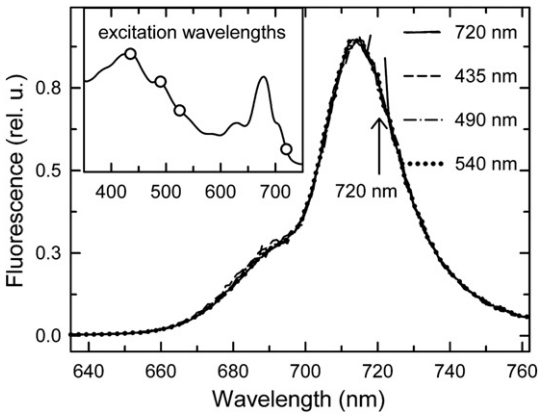

Fig. 9. Emission spectra of whole cells of *C. velia* grown under red-light (*C. velia-R*) measured at room temperature. Spectra were normalized at maximum. Excitation wavelengths are listed in legend and also marked in absorption spectrum of the cells (*Inset*). The emission spectrum excited at 720 nm was composed from separate measurement of uphill (<720 nm) and downhill (>720 nm) part. The points at 720 ± 1 nm were omitted from the measurement.

aggregates [67]. The relatively high amount of red chlorophyll is located in the core antenna of cyanobacterial PS I complexes [28,65] and in plant PS I light-harvesting complexes Lhca1/Lhca4 [28,68]. Here, we present several experimental proofs of functional connection of the red chlorophylls to PS II in *C. velia*. This is supported by a series of experimental data. Firstly, the F710 shows a variable fluorescence and induction character typical for PS II (see Fig. 7A). Although the similar conclusion has also been proposed for diatoms [9], no direct methods involving fluorescence variability were presented. Secondly, we clearly show the functional role of this PS II attached antenna complex, as oxygen evolution was clearly driven by near far-red light in *C. velia* (see Fig. 8B). The pronounced oxygen evolution induced by light above 700 nm has already been reported for coral associated alga *Ostreobium* sp. [24] that correlates well with the presence of a large number of red-shifted chlorophylls in this organism [22,23]. The far-red light induced stimulation of oxygen evolution was also documented for green alga *C. vulgaris* [29,30] and for plants [31–33] having a common chlorophyll *a*/*b* antennae. In the case of plants, far-red light driven PS II activity was proposed to be connected with the presence of red chlorophylls in the PS II antenna [31,32], but this idea is still a matter of debate [31,32,69,70]. Until now, the association of red chlorophylls with PS II has been conclusively

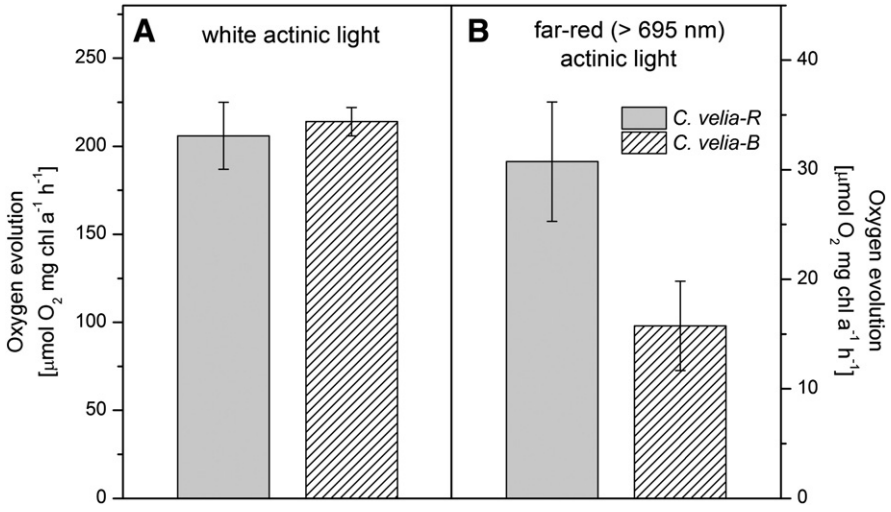

Fig. 8. Oxygen evolution rates of *C. velia* grown under red (*C. velia-R*) and blue (*C. velia-B*) continuous light measured with white (*Panel A*) and far-red >695 nm (*Panel B*) actinic light. Data represent averages and SD for n = 3.

proven only in two types of organisms. In *Ostreobium* sp., the red chlorophyll containing PS I antenna Lhca1 is atypically attached to PS II [23], which enables the uphill energy transfer from red chlorophylls to the RC of PS II [24]. In the moss *P. patens* antennae with red-shifted chlorophylls is represented by the LHCb9 protein [34] an antenna protein specific for mosses [35]. It seems that red-shifted light-harvesting proteins are characteristic for shade light-environments [71], a habitat typical for mosses like *P. patens*, for coral-reef associated organisms (*C. velia*, *Ostreobium* sp., *Acaryochloris*) and arguably also for other benthic [64] algae such as *Pheodactylum* and *Nitzschia*.

Another role played by the red-shifted antenna complexes functionally connected to PS II is that of photoprotection. It has been already suggested that far-red emitting fluorescence state could be related to a mechanism of non-photochemical quenching in higher plants [72,73] and in diatoms [74,75]. Furthermore, red chlorophyll molecules themselves play a significant role in photoprotection. This is well documented for cyanobacterial PS I trimers [65,76] and peripheral PS I antenna of plants [77]. However, red chlorophylls energetically coupled to PS II could provide an even more efficient and very fast dissipation pathway, as was discovered recently in desiccation tolerant mosses and lichens [78–81]. We have shown previously that the effective NPQ operates in *C. velia* that is dependent on violaxanthin de-epoxidation [82]. Here we have found a significant NPQ increase in the region around 710–720 nm in the *C. velia-R* variant (Fig. 7B). The *C. velia-R* cells also possess higher violaxanthin/Chl*a* ratio (Table 2). As the 17 kDa antenna binds violaxanthin (see accompanying paper [51]), we suggest that the Red-CLH complex forms an additional locus for NPQ.

All the factors mentioned above play a role in optimal chromatic adaptation of *C. velia* to light conditions in its natural environment. In nature, *C. velia* is associated with scleractinian corals [40,62] where it has to adapt to the two different light environments. This organism is not an obligate coral symbiont and in most cases it interacts with coral only indirectly through its association with the coral related macroalgae [47]. In this situation red light is attenuated by the water column and blue light dominates, which are conditions analogous to our *C. velia-B* variant. Moreover, *C. velia* is also able to live endosymbiotically within coral larvae [46] that shows its potential to live inside the coral tissue where the light microclimate is extremely poor in visible light but highly enriched in far-red [15] (comparable to *C. velia-R* variant in this work). We suggest that the capability of *C. velia* to thrive in such essentially different light environments has been brought about by effective chromatic adaptation of this organism.

Acknowledgements

This research project was supported by the Photosynthesis Research Center (GAČR P501/12/G055) financed by the Czech Science Foundation, by the project Algatech (CZ.1.05/2.1.00/03.0110) and by grant GAJU 134/2010/P. We thank Ingrid Romancová for the spectra deconvolution and Jason Dean for reading the manuscript.

References

[1] T. Mass, D.I. Kline, M. Roopin, C.J. Veal, S. Cohen, D. Iluz, O. Levy, The spectral quality of light is a key driver of photosynthesis and photoadaptation in *Stylophora pistillata* colonies from different depths in the Red Sea, J. Exp. Bot. 213 (2010) 4084–4091.
[2] F.A. Depauw, A. Rogato, M.R. d'Alcala, A. Falciatore, Exploring the molecular basis of responses to light in marine diatoms, J. Exp. Bot. 63 (2012) 1575–1591.
[3] S.G. Ackleson, Light in shallow waters: a brief research review, Limnol. Oceanogr. 48 (2003) 323–328.
[4] S. Maritorena, A. Morel, B. Gentili, Diffuse reflectance of oceanic shallow waters: influence of water depth and bottom albedo, Limnol. Oceanogr. 39 (1994) 1689–1703.
[5] P. Hegemann, Algal sensory photoreceptors, Annu. Rev. Plant Biol. (2008) 167–189.
[6] T.W. Engelmann, Farbe und Assimilation. I. Assimilation findet nur in den farbstoffhaltigen Plasmatheilchen statt. II. Näherer Zusammenhang zwischen Lichtabsorbtion und Assimilation. III.Weitere folgerungen, Bot. Ztg. (1883) 1–29.
[7] A. Gutu, D.M. Kehoe, Emerging perspectives on the mechanisms, regulation, and distribution of light color acclimation in cyanobacteria, Mol. Plant 5 (2012) 1–13.
[8] J.L. Mouget, P. Rosa, G. Tremblin, Acclimation of *Haslea ostrearia* to light of different spectral qualities — confirmation of 'chromatic adaptation' in diatoms, J. Photochem. Photobiol. B 75 (2004) 1–11.
[9] Y. Fujita, K. Ohki, On the 710 nm fluorescence emitted by the diatom *Phaeodactylum tricornutum* at room temperature, Plant Cell Physiol. 45 (2004) 392–397.
[10] E.S. Holdsworth, Effect of growth-factors and light quality on the growth, pigmentation and photosynthesis of 2 diatoms, *Thalassiosira gravida* and *Phaeodactylum tricornutum*, Mar. Biol. 86 (1985) 253–262.
[11] A. Morel, L. Lazzara, J. Gostan, Growth rate and quantum yield time response for a diatom to changing irradiances (energy and color), Limnol. Oceanogr. 32 (1987) 1066–1084.
[12] M.V. Nielsen, E. Sakshaug, Photobiological studies of *Skeletonema costatum* adapted to spectrally different light regimes, Limnol. Oceanogr. 38 (1993) 1576–1581.
[13] B.S. Costa, A. Jungandreas, T. Jakob, W. Weisheit, M. Mittag, C. Wilhelm, Blue light is essential for high light acclimation and photoprotection in the diatom *Phaeodactylum tricornutum*, J. Exp. Bot. 64 (2013) 483–493.
[14] S.J. Oh, D.I. Kim, T. Sajima, Y. Shimasaki, Y. Matsuyama, Y. Oshima, T. Honjo, H.S. Yang, Effects of irradiance of various wavelengths from light-emitting diodes on the growth of the harmful dinoflagellate *Heterocapsa circularisquama* and the diatom *Skeletonema costatum*, Fish. Sci. 74 (2008) 137–145.
[15] S.H. Magnusson, M. Fine, M. Kuhl, Light microclimate of endolithic phototrophs in the scleractinian corals *Montipora monasteriata* and *Porites cylindrica*, Mar. Ecol. Prog. Ser. 332 (2007) 119–128.
[16] M. Kuhl, M. Chen, P.J. Ralph, U. Schreiber, A.W.D. Larkum, A niche for cyanobacteria containing chlorophyll d, Nature 433 (2005) 820.
[17] D. Wangpraseurt, A.W. Larkum, P.J. Ralph, M. Kuhl, Light gradients and optical microniches in coral tissues, Front. Microbiol. 3 (2012) 316.
[18] M. Chen, R.E. Blankenship, Expanding the solar spectrum used by photosynthesis, Trends Plant Sci. 16 (2011) 427–431.
[19] H. Miyashita, H. Ikemoto, N. Kurano, K. Adachi, M. Chihara, S. Miyachi, Chlorophyll d as a major pigment, Nature 383 (1996) 402.
[20] H. Miyashita, K. Adachi, N. Kurano, H. Ikemoto, M. Chihara, S. Miyachi, Pigment composition of a novel oxygenic photosynthetic prokaryote containing chlorophyll d as the major chlorophyll, Plant Cell Physiol. 38 (1997) 274–281.
[21] M. Chen, M. Schliep, R.D. Willows, Z.L. Cai, B.A. Neilan, H. Scheer, A red-shifted chlorophyll, Science 329 (2010) 1318–1319.
[22] D.C. Fork, A.W.D. Larkum, Light harvesting in the green-alga *Ostreobium* sp., a coral symbiont adapted to extreme shade, Mar. Biol. 103 (1989) 381–385.
[23] B. Koehne, G. Elli, R.C. Jennings, C. Wilhelm, H.W. Trissl, Spectroscopic and molecular characterization of a long wavelength absorbing antenna of *Ostreobium* sp, Biochim. Biophys. Acta 1412 (1999) 94–107.
[24] C. Wilhelm, T. Jakob, Uphill energy transfer from long-wavelength absorbing chlorophylls to PSII in *Ostreobium* sp. is functional in carbon assimilation, Photosynth. Res. 87 (2006) 323–329.
[25] R.S. Gloag, R.J. Ritchie, M. Chen, A.W.D. Larkum, R.G. Quinnell, Chromatic photoacclimation, photosynthetic electron transport and oxygen evolution in the Chlorophyll d-containing oxyphotobacterium *Acaryochloris marina*, Biochim. Biophys. Acta 1767 (2007) 127–135.
[26] W.L. Butler, A far red absorbing form of chlorophyll, Biochem. Biophys. Res. Commun. 3 (1960) 685–688.
[27] W.L. Butler, A far-red absorbing form of chlorophyll, *in vivo*, Arch. Biochem. Biophys. 93 (1961) 413–422.
[28] B. Gobets, R. van Grondelle, Energy transfer and trapping in photosystem I, Biochim. Biophys. Acta 1507 (2001) 80–99.
[29] J. Myers, J.R. Graham, Enhancement in chlorella, Plant Physiol. 38 (1963) 105–116.
[30] N.L. Greenbaum, D. Mauzerall, Effect of irradiance level on distribution of chlorophylls between PS-II and PS-I as determined from optical-cross-sections, Biochim. Biophys. Acta 1057 (1991) 195–207.
[31] H. Pettai, V. Oja, A. Freiberg, A. Laisk, The long-wavelength limit of plant photosynthesis, FEBS Lett. 579 (2005) 4017–4019.
[32] H. Pettai, V. Oja, A. Freiberg, A. Laisk, Photosynthetic activity of far-red light in green plants, Biochim. Biophys. Acta 1708 (2005) 311–321.
[33] A. Thapper, F. Mamedov, F. Mokvist, L. Hammarstrom, S. Styring, Defining the far-red limit of photosystem II in spinach, Plant Cell 21 (2009) 2391–2401.
[34] A. Alboresi, C. Gerotto, S. Cazzaniga, R. Bassi, T. Morosinotto, A red-shifted antenna protein associated with photosystem II in *Physcomitrella patens*, J. Biol. Chem. 286 (2011) 28978–28987.
[35] A. Alboresi, S. Caffarri, F. Nogue, R. Bassi, T. Morosinotto, In silico and biochemical analysis of *Physcomitrella patens* photosynthetic antenna: identification of subunits which evolved upon land adaptation, Plos One 3 (2008) e2033.
[36] C.S. French, Changes with age in absorption spectrum of chlorophyll a in a diatom, Arch. Mikrobiol. 59 (1967) 93–103.
[37] S. Shimura, Y. Fujita, Some properties of chlorophyll fluorescence of diatom *Phaeodactylum tricornutum*, Plant Cell Physiol. 14 (1973) 341–352.
[38] J.S. Brown, Ffluorometric evidence for participation of chlorophyll a-695 in system 2 of photosynthesis, Biochim. Biophys. Acta 143 (1967) 391–398.
[39] K. Sugahara, N. Murata, A. Takamiya, Fluorescence of chlorophyll in brown algae and diatoms, Plant Cell Physiol. 12 (1971) 377–385.
[40] R.B. Moore, M. Obornik, J. Janouskovec, T. Chrudimsky, M. Vancova, D.H. Green, S.W. Wright, N.W. Davies, C.J.S. Bolch, K. Heimann, J. Slapeta, O. Hoegh-Guldberg, J.M. Logsdon, D.A. Carter, A photosynthetic alveolate closely related to apicomplexan parasites, Nature 451 (2008) 959–963.

[41] M. Obornik, M. Vancova, D.-H. Lai, J. Janouskovec, P.J. Keeling, J. Lukes, Morphology and ultrastructure of multiple life cycle stages of the photosynthetic relative of Apicomplexa, *Chromera velia*, Protist 162 (2011) 115–130.
[42] M. Obornik, D. Modry, M. Lukes, E. Cernotikova-Stribrna, J. Cihlar, M. Tesarova, E. Kotabova, M. Vancova, O. Prasil, J. Lukes, Morphology, ultrastructure and life cycle of *Vitrella brassicaformis* n. sp., n. gen., a novel chromerid from the Great Barrier Reef, Protist 163 (2012) 306–323.
[43] J. Janouskovec, A. Horak, M. Obornik, J. Lukes, P.J. Keeling, A common red algal origin of the apicomplexan, dinoflagellate, and heterokont plastids, Proc. Natl. Acad. Sci. U. S. A. 107 (2010) 10949–10954.
[44] K. Weatherby, D. Carter, *Chromera velia*: the missing link in the evolution of parasitism, Adv. Appl. Microbiol. 85 (2013) 119–144.
[45] M. Oborník, J. Lukeš, Cell biology of Chromerids: Autotrophic Relatives to Apicomplexan Parasites, 2013. 333–369.
[46] V.R. Cumbo, A.H. Baird, R.B. Moore, A.P. Negri, B.A. Neilan, A. Salih, M.J.H. van Oppen, Y. Wang, C.P. Marquis, *Chromera velia* is endosymbiotic in larvae of the reef corals *Acropora digitifera* and *A. tenuis*, Protist 164 (2013) 237–244.
[47] J. Janouskovec, A. Horak, K.L. Barott, F.L. Rohwer, P.J. Keeling, Environmental distribution of coral-associated relatives of apicomplexan parasites, ISME J. 7 (2013) 444–447.
[48] A. Quigg, E. Kotabova, J. Jaresova, R. Kana, J. Setlik, B. Sediva, O. Komarek, O. Prasil, Photosynthesis in *Chromera velia* represents a simple system with high efficiency, Plos One 7 (2012) e47036.
[49] H. Pan, J. Slapeta, D. Carter, M. Chen, Phylogenetic analysis of the light-harvesting system in *Chromera velia*, Photosynth. Res. 111 (2012) 19–28.
[50] J. Tichy, Z. Gardian, D. Bina, P. Konik, R. Litvin, M. Herbstova, A. Pain, F. Vacha, Light harvesting complexes of *Chromera velia*, photosynthetic relative of apicomplexan parasites, Biochim. Biophys. Acta 1827 (2013) 723–729.
[51] D. Bína, Z. Gardian, M. Herbstová, E. Kotabová, P. Koník, R. Litvín, O. Prášil, J. Tichý, F. Vácha, Novel type of red-shifted chlorophyll *a* antenna from *Chromera velia*. II. Biochemistry and spectroscopy, Biochim. Biophys. Acta 1837 (2014) 802–810(in this volume).
[52] R. Kana, O. Prasil, O. Komarek, G.C. Papageorgiou, Govindjee, spectral characteristic of fluorescence induction in a model cyanobacterium, *Synechococcus* sp (PCC 7942), Biochim. Biophys. Acta 1787 (2009) 1170–1178.
[53] R. Kana, E. Kotabova, O. Komarek, B. Sediva, G.C. Papageorgiou, Govindjee, O. Prasil, The slow S to M fluorescence rise in cyanobacteria is due to a state 2 to state 1 transition, Biochim. Biophys. Acta 1817 (2012) 1237–1247.
[54] R. Sobotka, U. Duhring, J. Komenda, E. Peter, Z. Gardian, M. Tichy, B. Grimm, A. Wilde, Importance of the cyanobacterial Gun4 protein for chlorophyll metabolism and assembly of photosynthetic complexes, J. Biol. Chem. 283 (2008) 25794–25802.
[55] I. Wittig, H. Schagger, Features and applications of blue-native and clear-native electrophoresis, Proteomics 8 (2008) 3974–3990.
[56] S.W. Jeffrey, R.F.C. Mantoura, S.W. Wright, Phytoplankton pigments in oceanography: guidelines to modern methods, second ed. UNESCO Publishing, Paris, 2005.
[57] R.J. Porra, The chequered history of the development and use of simultaneous equations for the accurate determination of chlorophylls a and b, Photosynth. Res. 73 (2002) 149–156.
[58] S.W. Wright, S.W. Jeffrey, Fucoxanthin pigment markers of marine phytoplankton analyzed by HPLC and HPTLC, Mar. Ecol. Prog. Ser. 38 (1987) 259–266.
[59] R. Kana, E. Kotabova, R. Sobotka, O. Prasil, Non-photochemical quenching in cryptophyte alga *Rhodomonas salina* is located in chlorophyll a/c antennae, Plos One 7 (2012) e29700.
[60] F. Bruyant, M. Babin, B. Genty, O. Prasil, M.J. Behrenfeld, H. Claustre, A. Bricaud, L. Garczarek, J. Holtzendorff, M. Koblizek, H. Dousova, F. Partensky, Diel variations in the photosynthetic parameters of *Prochlorococcus* strain PCC 9511: Combined effects of light and cell cycle, Limnol. Oceanogr. 50 (2005) 850–863.
[61] J. Janouskovec, R. Sobotka, D.H. Lai, P. Flegontov, P. Konik, J. Komenda, S. Ali, O. Prasil, A. Pain, M. Obornik, J. Lukes, P.J. Keeling, Split photosystem protein, linear-mapping topology and growth of structural complexity in the plastid genome of *Chromera velia*, Mol. Biol. Evol. 30 (2013) 2447–2462.
[62] J. Janouskovec, A. Horak, K.L. Barott, F.L. Rohwer, P.J. Keeling, Global analysis of plastid diversity reveals apicomplexan-related lineages in coral reefs, Curr. Biol. 22 (2012) R518–R519.
[63] H.W. Trissl, Long-wavelength absorbing antenna pigments and heterogenous absorption-bands concentrate excitons and increase absorption cross-section, Photosynth. Res. 35 (1993) 247–263.
[64] J. Serodio, J.M. daSilva, F. Catarino, Nondestructive tracing of migratory rhythms of intertidal benthic microalgae using in vivo chlorophyll a fluorescence, J. Phycol. 33 (1997) 542–553.
[65] N.V. Karapetyan, Protective dissipation of excess absorbed energy by photosynthetic apparatus of cyanobacteria: role of antenna terminal emitters, Photosynth. Res. 97 (2008) 195–204.
[66] M. Brecht, Spectroscopic characterization of photosystem I at the single-molecule level, Mol. Phys. 107 (2009) 1955–1974.
[67] S.S. Brody, New excited state of chlorophyll, Science 128 (1958) 839.
[68] S. Jansson, The light-harvesting chlorophyll a/b-binding proteins, Biochim. Biophys. Acta 1184 (1994) 1–19.
[69] H.W. Trissl, Comments to water-splitting activity of photosystem II by far-red light in green plants, Biochim. Biophys. Acta 1757 (2006) 155–157.
[70] H. Pettai, V. Oja, A. Freiberg, A. Laisk, Response to the "Comments to water-splitting activity of photosystem II by far-red light in green plant" by H.-W. Trissl, Biochim. Biophys. Acta 1757 (2006) 158–159.
[71] A. Rivadossi, G. Zucchelli, F.M. Garlaschi, R.C. Jennings, The importance of PSI chlorophyll red forms in light-harvesting by leaves, Photosynth. Res. 60 (1999) 209–215.
[72] Y. Miloslavina, A. Wehner, P.H. Lambrev, E. Wientjes, M. Reus, G. Garab, R. Croce, A.R. Holzwarth, Far-red fluorescence: a direct spectroscopic marker for LHCII oligomer formation in non-photochemical quenching, FEBS Lett. 582 (2008) 3625–3631.
[73] P.H. Lambrev, M. Nilkens, Y. Miloslavina, P. Jahns, A.R. Holzwarth, Kinetic and spectral resolution of multiple nonphotochemical quenching components in *Arabidopsis* leaves, Plant Physiol. 152 (2010) 1611–1624.
[74] Y. Miloslavina, I. Grouneva, P.H. Lambrev, B. Lepetit, R. Goss, C. Wilhelm, A.R. Holzwarth, Ultrafast fluorescence study on the location and mechanism of non-photochemical quenching in diatoms, Biochim. Biophys. Acta 1787 (2009) 1189–1197.
[75] J. Lavaud, B. Lepetit, An explanation for the inter-species variability of the photoprotective non-photochemical chlorophyll fluorescence quenching in diatoms, Biochim. Biophys. Acta 1827 (2013) 294–302.
[76] N.V. Karapetyan, A.R. Holzwarth, M. Rogner, The photosystem I trimer of cyanobacteria: molecular organization, excitation dynamics and physiological significance, FEBS Lett. 460 (1999) 395–400.
[77] D. Carbonera, G. Agostini, T. Morosinotto, R. Bassi, Quenching of chlorophyll triplet states by carotenoids in reconstituted Lhca4 subunit of peripheral light-harvesting complex of photosystem I, Biochemistry 44 (2005) 8337–8346.
[78] U. Heber, V.A. Shuvalov, Photochemical reactions of chlorophyll in dehydrated Photosystem II: two chlorophyll forms (680 and 700 nm), Photosynth. Res. 84 (2005) 85–91.
[79] J. Veerman, S. Vasil'ev, G.D. Paton, J. Ramanauskas, D. Bruce, Photoprotection in the lichen *Parmelia sulcata*: the origins of desiccation-induced fluorescence quenching, Plant Physiol. 145 (2007) 997–1005.
[80] H. Yamakawa, Y. Fukushima, S. Itoh, U. Heber, Three different mechanisms of energy dissipation of a desiccation-tolerant moss serve one common purpose: to protect reaction centres against photo-oxidation, J. Exp. Bot. 63 (2012) 3765–3775.
[81] M. Komura, A. Yamagishi, Y. Shibata, I. Iwasaki, S. Itoh, Mechanism of strong quenching of photosystem II chlorophyll fluorescence under drought stress in a lichen, *Physciella melanchla*, studied by subpicosecond fluorescence spectroscopy, Biochim. Biophys. Acta 1797 (2010) 331–338.
[82] E. Kotabova, R. Kana, J. Jaresova, O. Prasil, Non-photochemical fluorescence quenching in *Chromera velia* is enabled by fast violaxanthin de-epoxidation, FEBS Lett. 585 (2011) 1941–1945.